Three-dimensional kicked hydrogen atom

M. Klews and W. Schweizer
Institut für Astronomie und Astrophysik, Abteilung Theoretische Astrophysik, Universität Tübingen, D-72076 Tübingen, Germany
(Received 17 March 2001; published 2 October 2001)

We present an effective computational method and quantum results for the three-dimensional propagation of wave packets in the hydrogen atom driven by a train of short unidirectional electric-field pulses. We studied the dynamics of wave packets that are initially in a Stark state with different parabolic quantum numbers and observed quantum localization in the high-frequency domain.

DOI: 10.1103/PhysRevA.64.053403 PACS number(s): 32.80.Rm, 42.50.Hz, 05.45.Mt

I. INTRODUCTION

In the early 20th century, physicists realized that describing atoms in purely classical terms is doomed to failure. Since then, the connection between classical mechanics and quantum mechanics has interested researchers. The rich structure observed in low-dimensional nonintegrable classical systems has renewed and strengthened this interest and the study of highly excited atoms has put a fresh face on the connections between classical and quantum mechanics. Of particular interest is the study of quantum systems whose classical counterpart exhibits chaos. This situation is realized for the kicked hydrogen atom. This system consists of a hydrogen atom subject to a train of periodic field pulses, whose duration is short compared with the orbital period of the classical electron. The fascinating advantage of this system, is, in addition, that it could be treated both experimentally and, as we will show in this paper, computationally in the full three-dimensional space.

Over the past few years experimental results (see, e.g., [1,2]) have been compared with classical studies exhibiting a remarkable correspondence between classical and quantum systems. To date these classical theoretical studies have been mainly accompanied by a unidimensional treatment of the quantum system. For more details see, e.g., [1–7], and references therein. The experimental technique consisted of laser exciting an alkali-metal Rydberg electron with principal quantum number $n \approx 400$ and measuring its survival probability, which yields a good agreement with classical trajectory Monte Carlo simulations. For quantum dynamical calculations the quantum system was approximated by a one-dimensional model and [3] the wave function expanded in a large basis set of Sturmian pseudostates. With these calculations quantum localization was uncovered, a process which is typical for periodically driven systems like the kicked rotor [8,9].

The three-dimensional kicked quantum system has been treated [10] by a simple exactly solvable two-state, weak-field model due to numerical problems. Three-dimensional hydrogen Rydberg states, subject to a sequence of periodic and random pulses, have been studied in Ref. [11]. They used as basis expansion a superposition of hydrogen eigenstates and Sturmian states. The disadvantage of bound hydrogen eigenstates is, that for a complete description, the necessary continuum states are missing. This shortcoming could be partially overcome by using Sturmian eigenfunctions, because these functions built a complete basis without taken the continuum into account. Continuum states are no principle numerical problem for procedures based on space discretization techniques, as used in this paper. In Ref. [12] the three-dimensional (3D) kicked system with alternating pulses, has been studied. This is numerically simpler because due to the alternating pulses, the angular momentum remains significantly smaller compared to unidirectional pulses.

Our discretization method provides a convenient and accurate procedure for the propagation of wave packets in three dimensions. For the three-dimensional case it is based on a space discretization consisting of a combined discrete-variable and a finite-element scheme as described in Sec. II. This ansatz could be also combined with a suitable phenomenological potential, which mimics the multielectron core [13]. The time propagation will be solved by a time discretization based on a Cayley-like ansatz [14,15]. In Sec. III we compare our results with those presented in Ref. [10]. Quantum localization was found for the unidimensional approximation of the full quantum system [3]. Ever since then, the question arises if these findings are also true for the three dimensional system [16]. The answer could be provided by our method and some results will be shown in Sec. III. (The code is free and available upon request [17].)

II. METHOD

δ-shaped pulses are a widely used approximation for electric-field pulses that are much shorter than the classical orbital period. The Hamiltonian of the kicked hydrogen atom reads in atomic units

$$H = \frac{p^2}{2} - \frac{1}{r} + V_{\text{ext}} \quad \text{with} \quad V_{\text{ext}} = \mathbf{r}\cdot\mathbf{F}\sum_{k=0}^{S-1}\delta(t-kT), \tag{1}$$

where S is the number of kicks applied, T its period, and $\mathbf{F}$ is the external field. For a given pulse shape $\mathbf{F}(t)$ the momentum transfer integrated over the pulse duration is given by

$$\Delta\mathbf{p} = -\int \mathbf{F}(t)\,dt \tag{2}$$

and thus the external potential by

 ©2001 The American Physical Society

$$V_{\text{ext}} = -\mathbf{r}\cdot\Delta\mathbf{p}\sum_{k=0}^{S-1}\delta(t-kT). \tag{3}$$

Between the pulses we have a conservative system and the wave packet will be propagated due to the simple field free conservative Hamiltonian of the hydrogen atom. If the field-direction is the same for all pulses, e.g., along the $\hat{z}$ axis, we have rotational symmetry around this axis, and hence the corresponding component, here the z component, of the angular momentum is conserved. The electric field causes a strong coupling of bound states to the continuum leading to ionization. This is the main source of the computational challenge, but can be straightforwardly mastered by space-discretization methods. Due to the discretization the wave packet will not be approximated by a globally defined basis or by bound states and thus the well-known problem of finding a suitable bases ''simply'' reduces to selecting, first, a sufficiently large coordinate space, which allows wave packet propagation without reflection at the borders, and second, by selecting suitable interpolation polynomials on the space grid.

Between the pulses the wave packet evolves according to the time-dependent Schrödinger equation

$$H\psi(\mathbf{r},t) = i\frac{\partial\psi(\mathbf{r},t)}{\partial t}, \tag{4}$$

with $H=p^2/2-1/r$ the Hamiltonian of the field-free hydrogen atom. For the spatial integration we combined the discrete-variable method [18] with the finite-element technique, which has been successfully applied to various atomic systems in quest of astrophysical, quantumchaotical and wave-packet propagational problems (see, e.g., Refs. [14,19,15]). The wave function $\psi(\mathbf{r},t)$ is then represented by a set of N time-dependent functions

$$\psi_k(t) = \psi(\mathbf{r}_k,t), \quad k=1,\ldots,N, \tag{5}$$

and the Schrödinger equation (4) is mapped onto a system of coupled ordinary differential equations.

A formal solution for the time development of the discretized wave functions $\psi_k(t)$ evolving under a time-independent Hamiltonian is given by

$$\psi_k(t+\delta t) = e^{-iH\delta t}\psi_k(t). \tag{6}$$

The time propagator $e^{-iH\delta t}$ is approximated by a Cayley expansion

$$e^{-i\delta tH} \approx \left(1+\frac{i}{2}H\delta t\right)^{-1}\left(1-\frac{i}{2}H\delta t\right), \tag{7}$$

which preserves unitarity and is correct in order δt^2. Inserting Eq. (7) into Eq. (6) leads to an implicit system of algebraic equations

$$\left(1+\frac{i}{2}H\delta t\right)\psi_k(t+\delta t) = \left(1-\frac{i}{2}H\delta t\right)\psi_k(t), \tag{8}$$

which have to be solved for each time step δt.

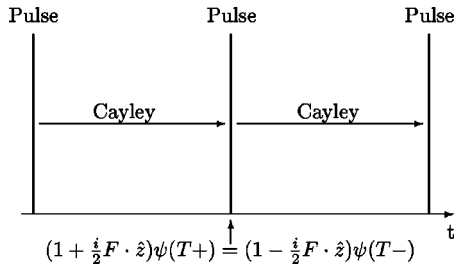

FIG. 1. Our time-integration scheme: between the pulses we use the Cayley method with the field-free hydrogen Hamiltonian. The wave function after the pulse $\psi(T+)$ can be calculated by solving $(1+i/2\mathbf{F}\cdot\hat{\mathbf{z}})\psi(T+)=(1-i/2\mathbf{F}\cdot\hat{\mathbf{z}})\psi(T-)$, with $\psi(T-)$ the wave function immediately before the pulse.

To explain the computational procedure for periodic δ pulses, we restrict the following discussion onto the Schrödinger equation for a single pulse directed along the z axis:

$$\frac{\partial\psi(\mathbf{r},t)}{\partial t} = -iH\psi(\mathbf{r},t) - i\mathbf{F}\cdot\hat{\mathbf{z}}\,\delta(t-T). \tag{9}$$

Several pulses are then simply computed by repeating the computational steps described below for a single pulse. Thus, the same method allows also to compute systems with non-periodic, in the time randomly distributed pulses, pulses of varying strength, or pulses directed in opposite directions.

The formal solution of Eq. (9) reads

$$\psi(\mathbf{r},t) = e^{-itH}\psi(\mathbf{r},0) + \int_0^t e^{-i(t-s)H}(-i\mathbf{F}\cdot\hat{\mathbf{z}})\psi(\mathbf{r},s) \times\delta(s-T)ds, \tag{10}$$

which yields after integration

$$\left(1+\frac{i}{2}\mathbf{F}\cdot\hat{\mathbf{z}}\right)\psi(T+) = \left(1-\frac{i}{2}\mathbf{F}\cdot\hat{\mathbf{z}}\right)\psi(T-), \tag{11}$$

with $\psi(\mathbf{r},T-)$ the wave function immediately before the pulse and $\psi(\mathbf{r},T+)$ directly after the pulse. This time-integration scheme is illustrated in Fig. 1. Equation (11) describes exactly the influence of a δ pulse onto the wave function independently from the strength F of this pulse. Thus the computational scheme is only approximated by the assumption that the kicked system can be described by δ pulses, by the necessarily finite discretization of the wave function and by propagating the wave function in between two pulses via the Cayley expansion, Eq. (8).

The electric field causes a strong coupling between bound states and the continuum. Therefore the integration radius has to be chosen with care to avoid elastic scattering at the integration border. To weaken this problem we have implemented a masking function as proposed in Ref. [20]. By this masking function, the tails of the wave packet that are drifting into the continuum, and thus would be elastically reflected at the integration border, are significantly damped out. The masking function is given by

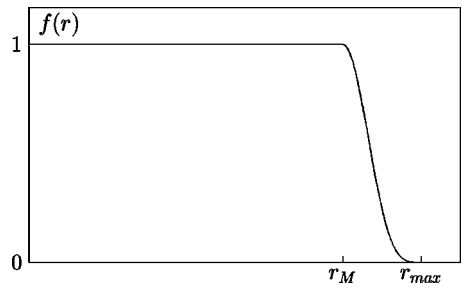

FIG. 2. To prevent reflections at the integration boundary the wave function is folded with the following masking function: $f(r) = \sin^4[\pi(r-r_{\max})/2(r_M-r_{\max})]$.

$$f(r)=\sin^4\left[\frac{\pi(r-r_{\max})}{2(r_M-r_{\max})}\right] \tag{12}$$

for r larger than the masking radius r_M, otherwise $f(r)=1$. The masking function is illustrated in Fig. 2. In our calculations we used mainly $(r_{\max}-r_M)/r_{\max}\approx 0.1$ and multiplied the wave packet with this masking function after each time step δt. With this method reflections at the integration border are prevented, but also parts of the wave packet that are correctly ''kicked'' back into the integration area by the electric pulses are as well damped out. By monitoring the norm of the wave packet after each computational step, we check if the integration radius is sufficiently large. Thus to obtain convergence, both, the size of the integration area and the size of the masking radius have to be carefully controlled.

III. RESULTS AND DISCUSSION

Dhar *et al.* [10] studied the time development of a parabolic Stark state with principal quantum number $n=9$, parabolic quantum number $k=0$, and $m=0$, see Fig. 3, under the influence of periodic pulses with a frequency equal to the transition frequency of the $n=9\rightarrow 10$ manifold. Thus the corresponding pulse period is $T=5357$. The selected field strength was $F=2\times 10^{-3}$. The computation was carried out in a small basis of bounded hydrogenic eigenstates. They obtained a resonance between the $n=9$ and $n=10$ states (n is the principal quantum number). This is uncovered in Fig. 4(a), in which we show the overlap of the propagated wave packet with the $n=9$ and $n=10$ manifold for fixed magnetic quantum number $m=0$. To compare our result with Ref. [10], we used exactly the same initial state, and for the readers' convenience the same notation on the left-hand side of Eq. (13). In the parabolic quantum number $|n,k,m\rangle$ this state is given by

$$|n=9\rangle=|9,0,0\rangle. \tag{13}$$

Our results are in exact agreement with their results (Ref. [10], Fig. 1), which gives added confidence in our method.

In addition we present in Fig. 4(b) the autocorrelation function $C(t)=|\langle\psi(t)|\psi(0)\rangle|$ for the parabolic $|nkm\rangle = |9,0,0\rangle$ state mentioned above and in Fig. 4(c) for a hydrogenic state with the quantum numbers $n=9$, $l=0$, and $m=0$. For the parabolic quantum number $k=0$, several l values are mixed and thus these two figures show the strong influence of the angular momentum distribution of the initial wave function on its time development. In Fig. 4(d) we have plotted the expectation value of the angular momentum as a function of the time for the hydrogenic $|900\rangle$ state. Due to the kicks, this wave packet exhibits a periodic behavior. At the maxima the wave packet is running through a nearly spherical shape. It is well known that constant electric fields have a weaker affect on spherical states (high angular momentum). Simplified, a similar behavior is also shown in Fig. 4(d) and thus the maxima (large angular momentum) are significantly broader than the minima. Thus, a wave packet with large angular momentum expectation value is less affected by the kicks compared to wave packets with small angular momentum.

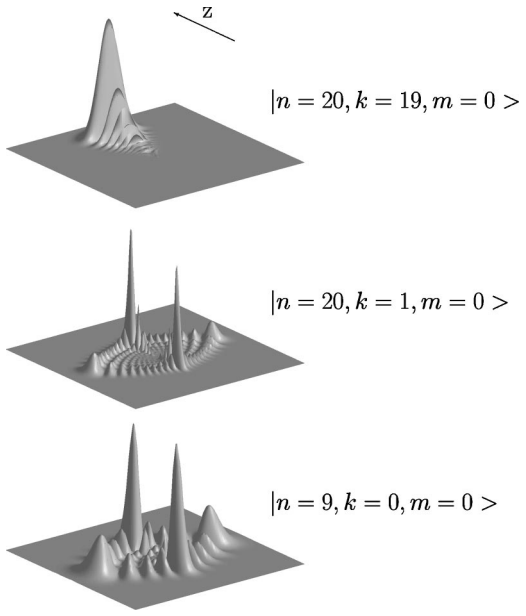

FIG. 3. The probability density of several Stark states. From top to bottom: $|nkm\rangle=|20,19,0\rangle$, $|20,1,0\rangle$, and $|9,0,0\rangle$. The higher the parabolic quantum number k, the stronger the localization along the **z** axis.

Reinhold *et al.* [3] studied the kicked atom in the high-frequency domain, with scaled frequency $\tilde{\nu}=16.8$. The frequency scales for the Coulomb problem with $\tilde{\nu}=\nu/n^3$, where n is the principal quantum number. By comparing one-dimensional classical and quantum-mechanical calculations they could uncover quantum localization. In the classical calculations the dynamics of an ensemble of particles, initially starting on different points in phase space but on the same torus, was computed.

In order to compare classical and quantum-mechanical calculations the question arises what quantum-mechanical state should be used for the initial wave packet? In unidimensional calculations, the particles move along a single axis. There is, of course, no other possibility. Therefore, to be as close as possible to the studies presented in Ref. [3], we used for comparison with the three-dimensional system, strongly on the z-axis, localized parabolic Stark states, thus with high parabolic quantum numbers. The probability den-

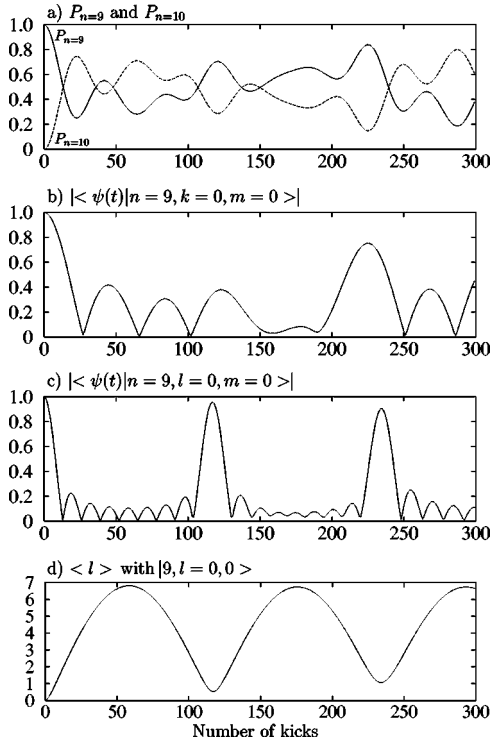

FIG. 4. The parabolic state $|nkm\rangle=|9,0,0\rangle$ and the hydrogenic state $|nlm\rangle=|9,0,0\rangle$ under the influence of a driving field with the frequency equal to the transition frequency between the $n=9$ and the $n=10$ states. (Field period $T=5357t_0$, field strength $F=2\times10^{-3}$). (a) The probabilities $\Sigma_{l=0}^{8}|\langle 9,l,0|\psi(t)\rangle|^2$ and $\Sigma_{l=0}^{9}|\langle 10,l,0|\psi(t)\rangle|^2$ with $|\psi(0)\rangle=|n=9\rangle$ [see Eq. (13)]. (b) The autocorrelation function $|\langle\psi(t)|n=9,k=0,m=0\rangle|$ and (c) the autocorrelation function $|\langle\psi(t)|n=9,l=0,m=0\rangle|$ in dependence of the number of kicks. (d) The expectation value of the angular momentum $\langle l\rangle(t)$ for the initial wave packet $|\psi_0\rangle=|n=9,l=0,m=0\rangle$.

sity of some Stark states is shown in Fig. 3. In Fig. 5 we present the recurrence probability for a series of different quantum numbers n, $k=n-1$, and $m=0$ in the high-frequency regime ($\tilde{\nu}=16.8$, $\Delta\tilde{p}=0.01$, the momentum scales with $\Delta\tilde{p}=\Delta p/n$). The cases $n=5$, $n=20$ and $n=50$ were studied for the 1D case in Ref. [3] and are almost indistinguishable from the 3D calculations for low principal quantum numbers. The higher the quantum number is, the larger the difference in the amplitudes of the autocorrelation function, while the frequency of the oscillations remain nearly unchanged. But obviously the same mechanisms of quantum localization occurs also in the three-dimensional case.

In Fig. 6 we show the autocorrelation function for several Stark states of the same *n*-manifold but with different parabolic quantum numbers. We used the same driving field as in Fig. 5. With decreasing parabolic quantum number *k*, the states become stronger located on the negative **z** axis. Locating the state on the negative **z** axis is the equivalent of locating the state on the positive **z** axis but using kicks with opposite field direction. For the one-dimensional system, the dynamics completely changed with the field direction [1]. By running through different parabolic quantum numbers one

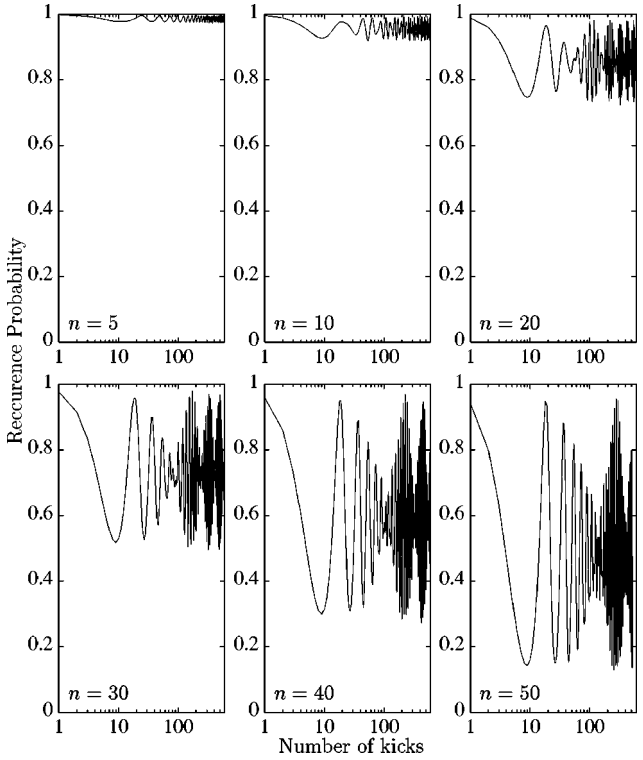

FIG. 5. The recurrence probability $|\langle\psi(t)|\psi_0\rangle|^2$ of some Stark states $|n,k=n-1,m=0\rangle$ for different principle quantum numbers $n=5$, 10, 20, 30, 40, and 50 under the influence of a high-frequency train of pulses with $\tilde{\nu}=16.8$ and $\Delta\tilde{p}=0.01$.

would thus naïvely expect a similar behavior, but this tremendous change observed in the one-dimensional system could not be observed here. Obviously there is one difference between a uni- and a multidimensional system. In a one-dimensional system the left-hand and the right-hand side is strictly separated by the Coulomb singularity. For multidi-

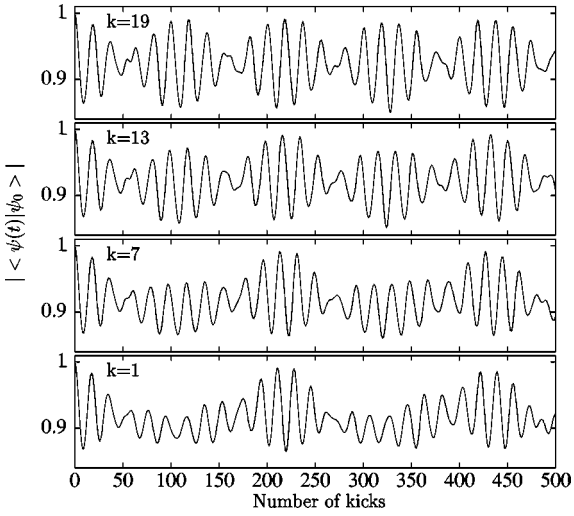

FIG. 6. The autocorrelation function for Stark states under influence of a high-frequency train of pulses with $\tilde{\nu}=16.8$ and $\Delta\tilde{p}=0.01$. The principle quantum number is $n=20$ and the parabolic quantum numbers $k=19$, 13, 7, and 1 (from top to bottom).

mensional systems this is no longer true. For the electron there is from the very beginning a nonzero probability of presence around the Coulomb singularity and thus not only a flux towards or away from the singularity, but also around the singularity. Hence there is a qualitative change by going from one-dimensional to multidimensional systems. Simplified, the electron has more kinematical possibilities to move in phase space, and can no longer be confined to one-half space by the Coulomb singularity. In addition the possibility to study states that are equally localized on both, the three-dimensional system offers the negative and the positive **z** axis and thus, driving the ''electron'' in the direction of the core on one side and against the core on the other side. Due to our discretization technique we could also synthesize any other shape for the initial wave packet [21].

By space discretization we were able to perform quantum-mechanical calculations for the three-dimensional kicked hydrogen atom. This method is fast converging and flexible. We already included phenomenological potentials to simulate the wave-packet propagation in alkali-metal atoms. A comparison with the results for hydrogen will be published elsewhere. Due to the space discretization in our method we are free to use any shape for the initial wave packet. The only limits are due to the available computer. All calculations presented here were performed on low-cost single-processor PC's with a maximum memory requirement of approximately 600 MB.

ACKNOWLEDGMENT

Discussions with C. Lubich are gratefully acknowledged.

[1] M. T. Frey, F. B. Dunning, C. O. Reinhold, S. Yoshida, and J. Burgdörfer, Phys. Rev. A **59**, 1434 (1999).
[2] B. E. Tannian, C. L. Stokely, F. B. Dunning, C. O. Reinhold, S. Yoshida, and J. Burgdörfer, Phys. Rev. A **62**, 043402 (2000).
[3] S. Yoshida, C. O. Reinhold, P. Kristöfel, and J. Burgdörfer, Phys. Rev. A **62**, 023408 (2000).
[4] T. P. Grozdanov and H. S. Taylor, J. Phys. B **20**, 3683 (1987).
[5] J. Burgdörfer, Nucl. Instrum. Methods Phys. Res. B **79**, 109 (1993).
[6] A. Carnegie, J. Phys. B **17**, 3435 (1984).
[7] C. F. Hillermeier, R. Blümel, and U. Smilansky, Phys. Rev. A **45**, 3486 (1992).
[8] S. Fishman, D. R. Grempel, and R. E. Prange, Phys. Rev. Lett. **49**, 509 (1982).
[9] E. Ott, *Chaos in Dynamical Systems* (Cambridge University, New York, 1993).
[10] A. K. Dhar, M. A. Nagaranjan, F. M. Izrailev, and R. R. Whitehead, J. Phys. B **16**, L17 (1983).
[11] M. Melles, C. O. Reinhold, and J. Burgdörfer, Nucl. Instrum. Methods Phys. Res. B **79**, 109 (1993).
[12] H. Wiedemann, J. Mostowski, and F. Haake, Phys. Rev. A **49**, 1171 (1994).
[13] J. Hannsen, R. McCarrol, and P. Valitron, J. Phys. B **12**, 899 (1979); W. Schweizer, P. Faßinder, and R. Gonzalez-Ferez, At. Data Nucl. Data Tables **72**, 33 (1999).
[14] W. Schweizer, P. Faßinder, R. Gonzalez-Ferez, M. Braun, S. Kulla, and M. Stehle, J. Comput. Appl. Math. **109**, 95 (1999).
[15] P. Faßinder, W. Schweizer, and T. Uzer, Phys. Rev. A **56**, 3626 (1997).
[16] S. Yoshida, C. O. Reinhold, and J. Burgdörfer, Phys. Rev. Lett. **84**, 2602 (2000).
[17] The codes available on request consist of FORTRAN codes for the space discretization, based on the discrete variable and finite-element method. For the finite-element method the radial coordinate is quadratically spaced and Lagrange interpolation polynomials of third order are used. The time discretization leads then to a system of linear equations. This system of linear equations has been solved by using Lapack routines. For efficiency control (time and storage), some simple C codes are additionally implemented.
[18] V. S. Melezhik, Phys. Rev. A **48**, 4528 (1993).
[19] P. Fassbinder and W. Schweizer, Phys. Rev. A **53**, 2135 (1996).
[20] S. Yoshida, S. Watanabe, C. O. Reinhold, and J. Burgdörfer, Phys. Rev. A **60**, 1113 (1999).
[21] W. Schweizer, W. Jans, and T. Uzer, Phys. Rev. A **58**, 1382 (1998); **60**, 1414 (1999).